Nanotechnology **19** (2008) 045303 (6pp) doi:10.1088/0957-4484/19/04/045303

Controlled synthesis of InAs wires, dot and twin-dot array configurations by cleaved edge overgrowth

Emanuele Uccelli, Max Bichler, Simon Nürnberger, Gerhard Abstreiter and Anna Fontcuberta i Morral[1]

Walter Schottky Institut, Technische Universität München, Am Coulombwall 3, 85748 Garching, Germany

E-mail: annafm@wsi.tum.de

Received 12 October 2007, in final form 31 October 2007
Published 4 January 2008
Online at stacks.iop.org/Nano/19/045303

Abstract
We present experimental results on the controlled synthesis of InAs ordered nanostructures with three different grades of complexity: nanowires, quantum dot arrays, and double quantum dot arrays. A model for the diffusion of In adatoms on (110) surfaces explains the observed ordering and establishes general criteria for the optimized fabrication of the three different InAs nanostructure configurations, as a function of the growth conditions. These results are important for the use of ordered InAs nanostructures in future optoelectronic applications.

S Supplementary data are available from stacks.iop.org/Nano/19/045303

(Some figures in this article are in colour only in the electronic version)

Self-assembled quantum dots (QDs) have been extensively studied in the past decade because of their unique properties, which are mainly derived from the strong carrier confinement, leading to discretization of the electronic energy levels [1]. In this context, QDs are nanostructures that are expected to have great impact on optoelectronic devices in this century [2]. Methods to control the size and therefore the emission properties of QDs have been successfully developed, but the control of position has shown to be a more challenging task. QDs usually nucleate randomly on a substrate by self-assembly. Methods for controlling the position are based on inducing a preferential nucleation of the self-organized dots at certain points of a surface. Approaches range from the use of lithographically patterned substrates [3–6], to vicinal surfaces [7–11]. A novel concept for spatial control of the nucleation of InAs QDs is the use of the *in situ* cleaved edge overgrowth (CEO) method, which was used for the first time in 1990 by Pfeiffer *et al* [12] to fabricate electrostatically defined quantum wires. The main principle of the *in situ* CEO technique is to grow on a surface that has been freshly cleaved *in situ* in the molecular beam epitaxy (MBE) machine. It is common that the initial substrate will present one or several quantum well (QW) structures in the (001) direction. As a consequence of cleaving, the QW structures transform into stripes on a (110) facet. Here it is important to note that (110) is a natural cleavage plane in the GaAs system, meaning that these are the usual surface planes on which CEO growth is realized. After duly growing on the freshly cleaved facet, the stripes are transformed into electrostatically defined quantum wires or even QDs if a second cleave process in the perpendicular direction is realized [13]. Due to the fact that the quantum structures originate at the intersection of two or three quantum wells (which can be defined with atomic precision), one of the main advantages of the CEO for the fabrication of quantum structures is that their dimension can be defined with the atomic precision of MBE. Moreover, the quantum heterostructures are perfectly embedded in a semiconductor matrix, meaning that the intrinsic properties, without the influence of surface states, can be easily studied. This makes CEO quantum structures the model for understanding other types of one-dimensional nanostructures, such as nanowires, that may be less perfect from the morphological and geometrical point of view. Nanowires are free standing one-dimensional nanostructures. Their large non-capped surface can have a large influence on their final optical and electronic properties. This is why they

[1] Author to whom any correspondence should be addressed.

 © 2008 IOP Publishing Ltd Printed in the UK

are considered to be less perfect than electrostatically defined quantum wires.

In this paper, we present the growth of three types of well defined InAs ordered nanostructures obtained by the cleaved edge overgrowth method: wires, quantum dot arrays and double quantum dot arrays. In previous works, it has been demonstrated that, on GaAs/AlAs (110) surfaces, InAs tends to selectively accumulate on AlAs regions in the form of quantum dots [14]. However, InAs tends to form large triangular islands on (110) GaAs regions [15–17]. In this paper, after first outlining the mechanisms for selective formation of InAs nanostructures on (110) AlAs stripes, we show how the InAs arrangement can be mastered to achieve novel InAs nanostructure configurations, such as wires, QD arrays and double QD arrays. Finally, the geometry of the surface and the growth conditions are optimized for the selective formation of nanostructures only on the AlAs stripes, while avoiding the formation of defective islands on the GaAs regions.

In order to understand the nucleation and growth of InAs nanostructures, we analyzed the role of the geometry of the GaAs/AlAs cleaved surface on the morphology of the InAs nanostructures. The main idea behind these experiments was to prove and understand the parameters for the selective mass redistribution of InAs towards the AlAs stripes. We propose that the mass redistribution is a consequence of the significantly reduced mobility and lifetime of the adatoms on the (110) AlAs surface in comparison to the GaAs counterpart [18–21]. In a naive image, a significantly reduced mobility means that the In(As) adatoms will 'slow down' over the AlAs regions, which increases the probability of the adatoms precipitating and binding covalently on the surface. The consequence is that the amount (thickness) of InAs material deposited on the AlAs regions is larger than the nominal InAs thickness, and will depend on the stripe width. As will be shown, another consequence is that the onset for the formation of InAs QDs will depend on the AlAs stripe width. These two phenomena are unusual to standard MBE growth and open up the possibility of creating new forms of nanostructures.

In our growth studies, the cleaved (110) surface consisted of a series of AlAs stripes embedded in 90 nm GaAs spacers. The width of the AlAs regions was varied from 3 to 42 nm with a 3 nm increment in step size. First we investigated the onset of QD formation for the different AlAs stripe thicknesses as a function of the nominal InAs thickness. The nominal thickness is defined as the amount of material that would epitaxially grow on a lattice matched substrate, in number of monolayers (MLs), one ML being 2.83 Å. The surface morphology of the deposited samples was analyzed by atomic force microscopy (AFM). In figure 1, a three-dimensional representation of a typical AFM measurement of the surface after deposition of nominal 1.0 ML InAs is presented. The measurement is taken on the (110) regions where AlAs stripes with increasing thickness are present. Longitudinal wire-like structures with different heights are observed, with identical periodicity to the AlAs stripes. They can be identified as the InAs nanostructures formed on the AlAs stripes after cleavage of the (110) surface and subsequent InAs deposition. The surface in the GaAs

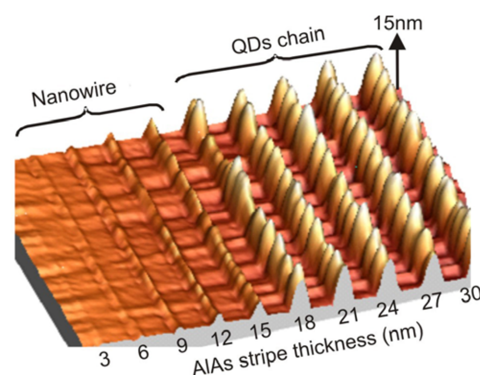

Figure 1. Three-dimensional atomic force micrograph of a cleaved facet with AlAs stripes of widths from 3 to 30 nm, after having nominally grown 1.0 ML of InAs. The formation of InAs nanowire structures on AlAs stripes narrower than 15 nm and InAs QD chains on larger AlAs stripes is observed.

spacing regions is completely flat, indicating that there is no apparent deposition in those regions. The height of the InAs nanostructures increases with AlAs width. Additionally, two different kinds of nanostructures are observed: on some stripes, the height along the (110) direction is homogeneous (wire), while on other stripes, the material aggregates, forming islands (QDs). The formation of QDs tends to occur on thicker stripes. As will be shown, this could, in principle, be explained through the Stranski–Krastanov mechanism (SK) [22]. The InAs and AlAs(GaAs) system is lattice mismatched, which results in a strain of the hetero-epitaxial layers. After a certain grown thickness, the built-in strain is released through the formation of small islands, QDs, or through the formation of dislocations [23]. On (110) surfaces, it has been shown that InAs QDs form only on AlAs surfaces [20]. In contrast, on (110) GaAs or $Al_xGa_{1-x}As$ surfaces ($x < 0.45$), the strain is released through highly dislocated macroscopic islands [21]. The onset for the formation of QDs on mismatched substrates typically is inversely proportional to the lattice mismatch. For example, in (001) GaAs surfaces, 1.6–1.7 ML of InAs is enough for the nucleation of InAs QDs [24, 25]. In our particular system, due to the preferential accumulation of InAs on AlAs stripes, the total thickness of InAs on the AlAs stripes is larger than the nominal thickness. The immediate consequence is that the onset of QD formation necessarily has to occur at a lower InAs nominal thickness than in the planar case.

In the following we analyze the transition of the InAs configurations from wire to quantum dot arrays. For that, we investigate the onset of QD nucleation as a function of the InAs nominal thickness. In figure 2, AFM measurements on the same kind of surfaces with three different nominal InAs thicknesses are shown. For simplicity, only the set of stripes containing the transition to QD formation are shown. From the top to the bottom of the figure, the measurements correspond to samples grown with respectively 3.2, 2.0 and 1.0 nominal MLs of InAs. The color code indicates the relative height of the structures. Again, chains with heights from 10 to 25 nm are observed, with identical periodicity to the AlAs stripes. Typically, Stranski–Krastanov type QDs present a

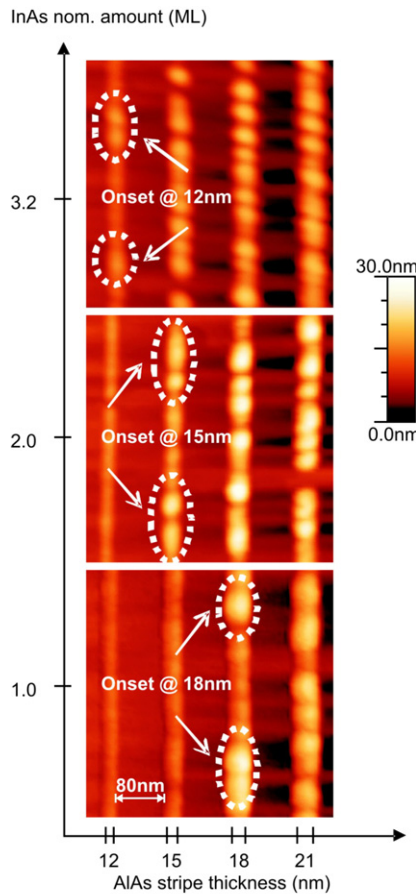

Figure 2. Atomic force micrograph of a cleaved (110) surface, patterned by AlAs stripes of thickness from 12 to 21 nm after growing three different InAs nominal thicknesses. The onset for quantum dot nucleation depends on the AlAs stripe thickness and the InAs nominal thickness.

lens-like shape, in which the height is much lower than the diameter [26, 27]. The formation of QDs with a nearly semi-spherical shape is striking, and may indicate the existence of a slightly different nucleation mechanism. As in figure 1, wires and QD arrays are observed (QDs at the nucleation onset for each sample are indicated with dashed circles). In agreement with what has been presented above, the onset of QD formation occurs on the thicker stripes. Moreover, we also observe that the onset of QD formation moves towards smaller AlAs stripe widths when the nominal InAs thickness is increased, which can be explained as follows. Let us assume that the critical thickness of InAs for QD formation is t_c. The amount of InAs on the AlAs stripe ($\boldsymbol{h}$) is proportional to the nominal InAs thickness (**ML**) and to the AlAs stripe width ($\boldsymbol{d}$): $h \propto \mathrm{ML} \cdot d$. This relation means that, for the nucleation of QD occurring at a given value of $h = t_c$, if MLs are decreased, then d has necessarily to increase.

In this section, we quantify the results presented in figures 1 and 2, relate them to our growth model, provide a more detailed understanding of the formation mechanism of the InAs nanostructures, and predict the formation of new structures. The average dimension of the quantum dots (wire) was analyzed along each stripe as a function of the AlAs stripe thickness, d, and the nominal InAs thickness. The results

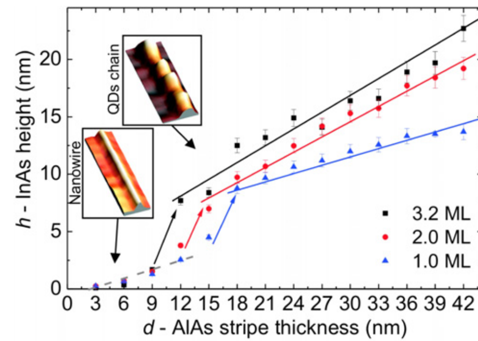

Figure 3. Average height of the InAs nanostructure arrays as a function of the thickness of the AlAs stripe, for three different InAs nominal thicknesses. A linear relation is found, with two main regimes, having different slopes corresponding to the arrangement of the deposited InAs in the form of nanowire or quantum dot array.

are presented in figure 3. The relation between height of the QDs, h and d is linear and presents two different regimes with different slopes. At small d values, h increases with a slope of 0.25 ± 0.05. After a certain onset there is a jump in the value of h and the second slope depends on the amount of InAs deposited. The transition occurs exactly at the point where the InAs nanostructures transform from wire to QD array geometry. It is also important to note that the height of the QDs in all cases is significantly larger than the nominal thickness deposited, indicating a strong migration of InAs from the neighboring areas, within the diffusion length distance ($\sim$1 μm on (110) GaAs). In a first order approximation, this allows us in the model to only consider one stripe and neglect the effect of the neighboring stripes. In fact, the same topology is observed for single stripe and multiple stripe geometries. The linear relation between h and d is a consequence of the lower mobility of In adatoms on (110) AlAs surfaces and, considering a very simplified one-dimensional model, follows [28]:

$$h \approx \frac{d}{\tau_{\mathrm{AlAs}} \cdot D_{\mathrm{AlAs}}} \cdot L_{\mathrm{GaAs}} \cdot ML = d \cdot \left(\frac{L_{\mathrm{GaAs}}}{L^2_{\mathrm{AlAs}}} \right) \cdot ML \quad (1)$$

where ML is the number of nominal InAs monolayers deposited, D_{AlAs} and τ_{AlAs} are the effective diffusion coefficient and lifetime of In adatoms on (110) AlAs stripes, and L_{AlAs} and L_{GaAs} are respectively the diffusion length of the In adatom on AlAs and GaAs surfaces. Following equation (1) and in agreement with the experimental results, the height increases with the number of MLs. The slope of the curve h versus d depends on the In adatom diffusion length on both GaAs and AlAs surfaces but in a different way. It is directly proportional to the indium diffusion length on the GaAs surface, while it is inversely proportional to the square of the indium diffusion length on the AlAs surface. Due to the deposition process, the value of the slope is a convolution of the diffusion length on (110) oriented AlAs stripes and on the growing InAs layers. The slope is slightly lower for the samples grown with 1.0 ML. This could be due to the fact that at 1 ML the diffusion length contains a higher contribution of the diffusion on bare AlAs, while at higher MLs the diffusion on InAs becomes predominant.

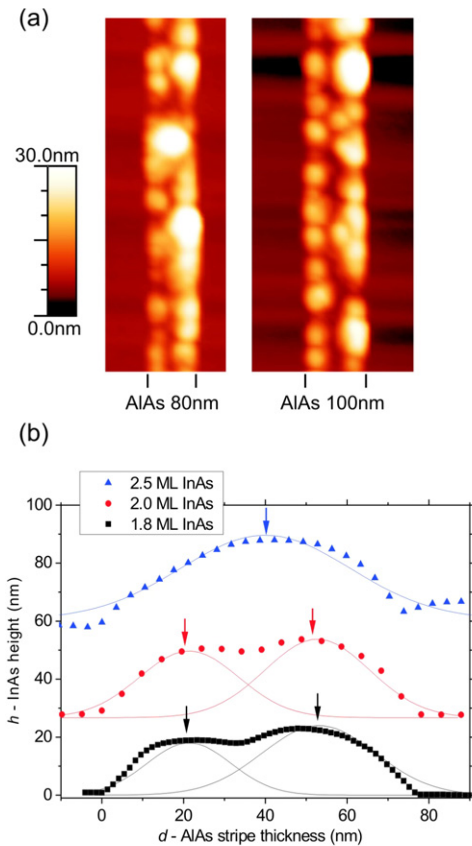

Figure 4. Extension of the InAs selective growth on thicker stripes (a) atomic force micrograph of a double QD chain nucleated on 80 and 100 nm wide AlAs stripes. (b) Dependence of double QDs on the nominal amount of deposited material, showing the transition from double dots into a big single dot.

The existence of two different behaviors before and after QD nucleation in the relation between h and d can be explained as a purely geometrical effect. Assuming the shape of the wires and QDs respectively as triangular prisms and cylindrical pyramids, all with base (diameter) d and height h, the volume is written as:

$$V_{\rm dot} = \frac{\pi}{3} \cdot \left(\frac{d}{2}\right)^2 \cdot h_{\rm dot} \tag{2}$$

$$V_{\rm wire} = \tfrac{1}{2} \cdot d^2 \cdot h_{\rm wire}. \tag{3}$$

This means that for the same amount of material and diameter d, when distributed into dots or wires, the height is 1.9 times higher in the case of the dots. There should therefore be a step in height of this factor after the transition, and the slope should consequently increase by a similar amount. As indicated in figure 3, the transition from wire to dot configuration has an intermediate stage, in which we find a slightly roughened wire.

In order to better understand the nucleation of QDs on the (110) AlAs stripes, the InAs deposition on wider AlAs stripes was investigated. Indeed, if the nucleation was pure SK mechanism, at larger widths one should observe a transition towards random QD nucleation through the stripe. Figure 4 shows the growth results on 80 and 100 nm AlAs stripes after deposition of 2.0 MLs of InAs. Clearly, one observes the nucleation of a dual chain of quantum dots. The nucleation is taking place preferentially at the AlAs/GaAs interface, which means that the nucleation mechanism in this kind of QD differs from the typical SK mechanism. Deposition of 1.8, 2.0, and 2.5 MLs of InAs was realized on the same stripes. The AFM profiles of the resulting surfaces of the 80 nm stripe are plotted in figure 4. After depositing 2.5 MLs of InAs, 80 nm wide QDs are observed. From the AFM profiles at thinner depositions, it is clear, however, that the QDs arise from the coalescence of double QDs. This further confirms a slightly different mechanism from SK; indeed, the QD nucleation seems to originate not only from the lattice mismatch strain, but also from the strain present at the AlAs/GaAs interface. For the sake of providing a more clear picture of the growth

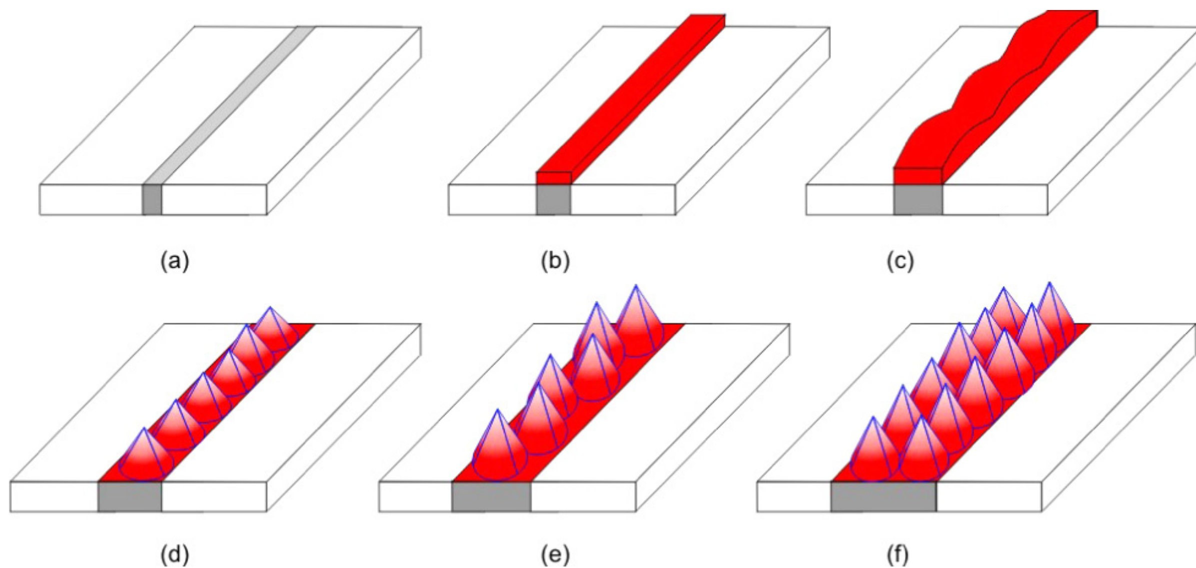

Figure 5. Schematic diagram of the possible growth mechanisms of InAs on (110) GaAs/AlAs facets, depending on the width of the underlying AlAs stripes.

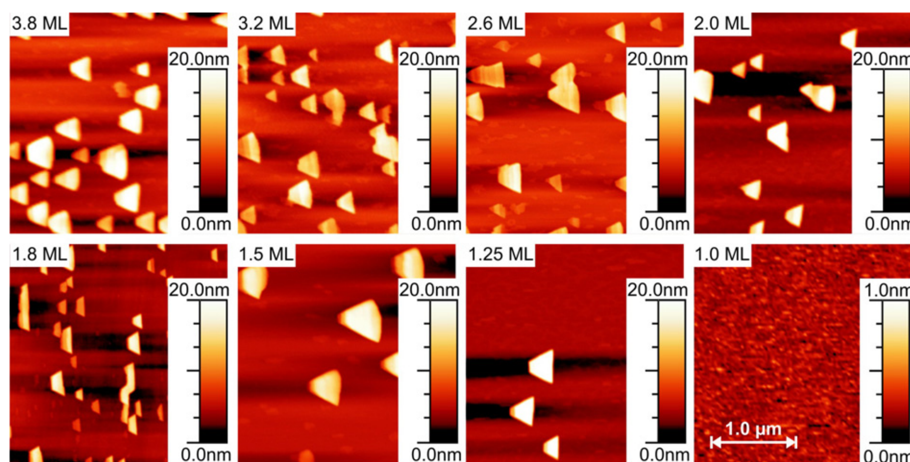

Figure 6. Atomic force micrographs showing the occurrence of InAs triangular defect density on (110) GaAs surfaces, as a function of the InAs nominal thickness. The nucleation of defects is avoided only at a nominal thickness of 1.0 ML.

mechanism for InAs nanostructures on (110) AlAs stripes, a schematic diagram for the selective InAs deposition model as a function of the nominal thickness is presented in figure 5.

Finally, we would like to present the growth results on the (110) GaAs regions. Even if InAs tends to accumulate preferentially on the AlAs stripes, leaving the neighboring GaAs areas free of deposition, there is still some deposition of InAs on GaAs in the form of large triangular islands. These InAs structures strongly perturb the InAs arrangements, which could hinder their use as functional nanostructures. In figure 6 we show AFM measurements of the (110) GaAs surfaces after growth of 1.0–3.8 MLs of InAs. Clearly, at larger deposition thickness, a higher density of triangular islands appears. When the nominal thickness is decreased to 1.0 ML, the surface is free of any triangular islands. InAs nanostructures are still observed on the AlAs stripes, giving an optimal condition for the completely selective fabrication of InAs nanostructures. InAs nucleates only on AlAs stripes, the geometry being controlled by the AlAs stripe width.

To conclude, we have presented a novel MBE method for the fabrication of three types of nanostructures: wires, quantum dot arrays, and dual chains of quantum dots. We have presented a theoretical model that fits the experimental results and has allowed the prediction of novel InAs nanostructure arrangements. Thanks to the MBE precision and crystalline quality, the present method allows the control of morphology at the atomic level, and therefore opens a new avenue for fundamental studies of InAs nanostructures.

Acknowledgments

This work was financially supported by the Deutsche Forschungsgemeinschaft (DFG) in the framework of SFB 631 TP B1, by the Bundesministerium für Bildung, Wissenschaft, Forschung und Technologie (BmBF) through the Grant NanoQUIT-01BM469, by the Marie Curie Excellence Grant ‘SENFED’ and by the Nanosystems Initiative München (NIM) of the DFG.

References

[1] Bimberg D, Grundmann M and Ledentsov N N 1998 *Quantum Dot Heterostructures* (New York: Wiley)
[2] Grundmann M 2001 *Nano-Optoelectronics: Concepts, Physics and Devices* (Berlin: Springer)
[3] Lee J H, Wang Z M, Black W T, Kunets V P, Mazur Y I and Salamo G J 2007 *Adv. Funct. Mater* **17** 3187
[4] Wang Z M, Lee J H, Liang B L, Black W T, Kunets V P, Mazur Y I and Salamo G J 2006 *Appl. Phys. Lett.* **88** 233102
[5] Lee J H, Wang Z M, Liang B L, Black W T, Kunets V P, Mazur Y I and Salamo G J 2006 *Nanotechnology* **17** 2275
[6] Songmuang R, Kiravittaya S and Schmidt O G 2003 *Appl. Phys. Lett.* **82** 2892
[7] Leon R, Chaparro S, Johnson S R, Navarro C, Jin X, Zhang Y H, Siegert J, Marcinkevicius S, Liao X Z and Zou J 2002 *J. Appl. Phys.* **91** 5826
[8] Bhat R, Kapon E, Hwang D M, Koza M A and Yun C P 1988 *J. Cryst. Growth* **93** 850
[9] Gerardot B D, Subramanian G, Minvielle S, Lee H, Johnson J A, Schoenfeld W V, Pine D, Speck J S and Petroff P M 2002 *J. Cryst. Growth* **236** 647
[10] Nötzel R and Ploog K H 2001 *J. Cryst. Growth* **227/228** 8
[11] Kim H J, Park Y J, Park Y M, Kim E K and Kim T W 2001 *Appl. Phys. Lett.* **78** 3253
[12] Pfeiffer L, West K W, Stormer H L, Eisenstein J P, Baldwin K W, Gershoni D and Spector J 1990 *Appl. Phys. Lett.* **56** 1697
[13] Schedelbeck G, Wegscheider W, Bichler M and Abstreiter G 1997 *Science* **278** 1792
[14] Bauer J, Schuh D, Uccelli E, Schulz R, Kress A, Hofbauer F, Finley J J and Abstreiter G 2004 *Appl. Phys. Lett.* **85** 4750
[15] Munekata H, Chang L L, Woronick S C and Kao Y H 1987 *J. Cryst. Growth* **81** 237
[16] Zhang X, Pashley D W, Hart L, Neave J H, Fawcett P N and Joyce B A 1983 *J. Cryst. Growth* **131** 300
[17] Belk J G, Pashley D W, Joyce B A and Jones T S 1998 *Phys. Rev.* B **58** 16194
[18] Baklenov O, Huffaker D L, Anselm A, Deppe D G and Streetman B G 1997 *J. Appl. Phys.* **82** 6362
[19] Ballet P, Smathers J B, Yang H, Workman C L and Salamo G J 2001 *J. Appl. Phys.* **90** 481
[20] Wasserman D, Lyon S A, Hadjipanayi M, Maciel A and Ryan J F 2003 *Appl. Phys. Lett.* **83** 5050
[21] Lobo C and Leon R 1998 *J. Appl. Phys.* **83** 4168
[22] Stranski I N and Krastanow L 1938 *Sitz. Akad. Wiss. Math.-Nat. Kl. 2b* **146** 797

[23] Shchukin V A, Ledentsov N N and Bimberg D 2004 *Epitaxy of Nanostructures* (Berlin: Springer)
[24] Goldstein L, Glas F, Marzin J Y, Charasse M N and Le Roux G 1985 *Appl. Phys. Lett.* **47** 1099
[25] Kobayashi N P, Ramachandran T R, Chen P and Madhukar A 1996 *Appl. Phys. Lett.* **68** 3299
[26] Moison J m, Houzay F, Barthe F, Leprince L, André E and Vatel O 1994 *Appl. Phys. Lett* **64** 196
[27] Lee J H, Wang Z M, Liang B L, Sablon K A, Strom N W and Salamo G J 2006 *Semicond. Sci. Technol.* **21** 1547
[28] Uccelli E *et al* 2007 *Superlattices Microstruct.* submitted